Supporting Information

Revising the common understanding of metamagnetism in the molecule-based bisdithiazolyl BDTMe compound

Clàudia Climent,[a,b] *Sergi Vela,*[a,c] *Joaquim Jornet-Somoza,*[a,d] *Mercè Deumal*[a,]*

[a] Secció Química Física, Dept. Ciència de Materials i Química Física & IQTCUB, Universitat de Barcelona, Martí i Franquès 1, Barcelona, E-08028

[b] Departamento de Física Teórica de la Materia Condensada, Universidad Autónoma de Madrid, E-28049 Madrid

[c] Laboratory for Computational Molecular Design (LCMD), Institute of Chemical Sciences and Engineering, EPFL, CH-1015 Lausanne, Switzerland

[d] Theory Department, The Max Planck Institute for the Structure and Dynamics of Matter (MPSD), Bldg. 99 (CFEL), Luruper Chaussee 149, 22761 Hamburg, Germany

Section 1 - d1-d10 isolated pairs of BDTMe radicals

The geometry of the ten isolated pairs of BDTMe radicals is displayed below (see inset for shortest S···S contacts and for crystallographic axes for pair orientation).

d1

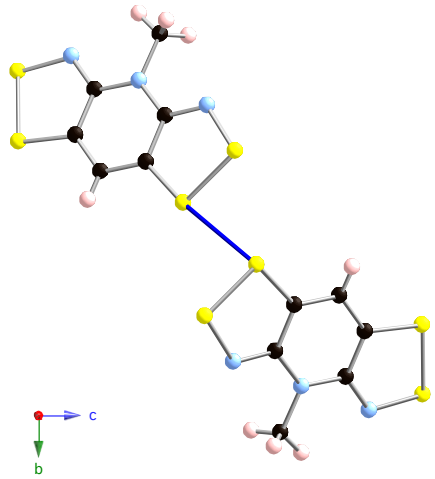

$d(S\cdots S)^{35K}_{min}$ = 3.355 Å; $d(S\cdots S)^{100K}_{min}$ = 3.361 Å

d4

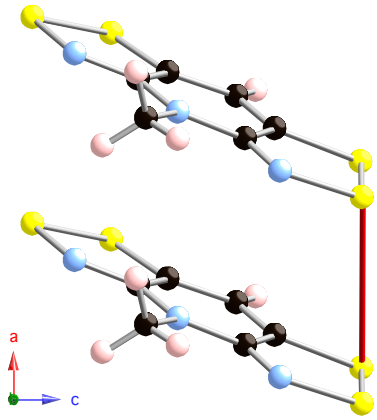

$d(S\cdots S)^{35K}_{min}$ = 3.779 Å ; $d(S\cdots S)^{100K}_{min}$ =3.776

d2

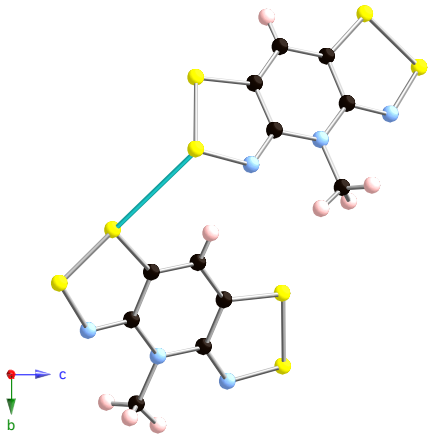

$d(S\cdots S)^{35K}_{min}$ = 3.337 Å; $d(S\cdots S)^{100K}_{min}$ = 3.334 Å

d5

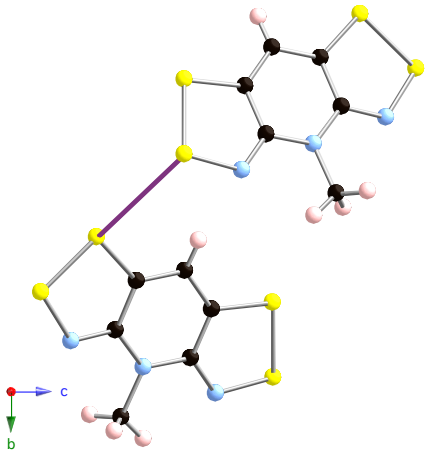

$d(S\cdots S)^{35K}_{min}$ = 5.817 Å; $d(S\cdots S)^{100K}_{min}$ = 5.843 Å

d3

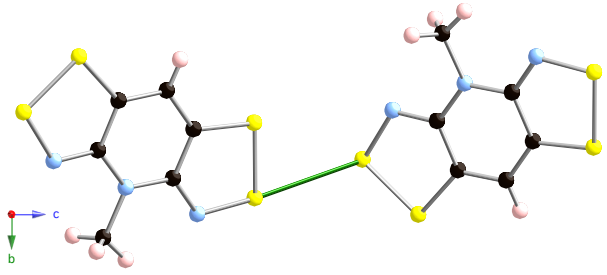

$d(S\cdots S)^{35K}_{min}$ = 3.329 Å; $d(S\cdots S)^{100K}_{min}$ = 3.325 Å

d7

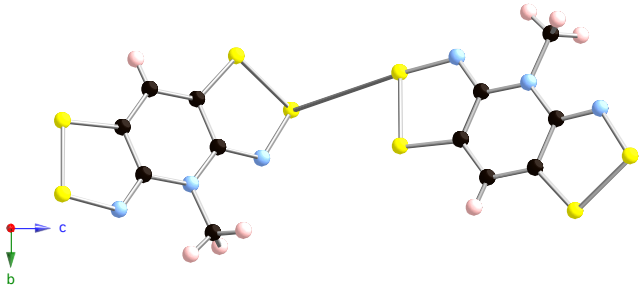

$d(S\cdots S)^{35K}_{min}$ = 5.996 Å; $d(S\cdots S)^{100K}_{min}$ = 5.973 Å

d6

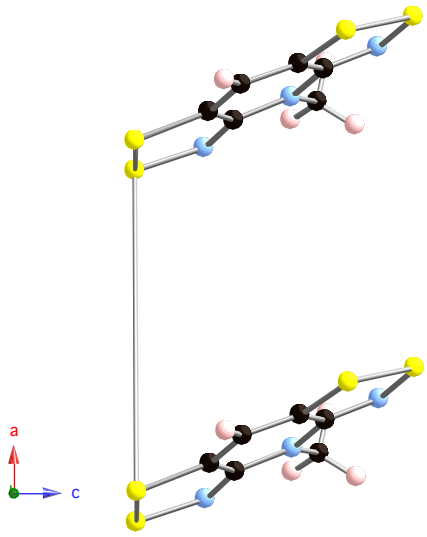

$d(S\cdots S)_{min}^{35K} = 7.367$ Å; $d(S\cdots S)_{min}^{100K} = 7.382$ Å

d8

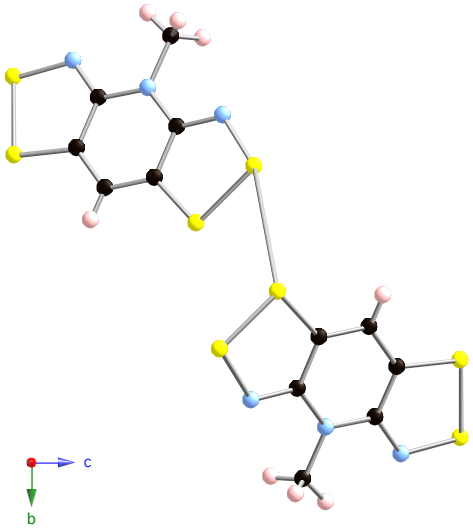

$d(S\cdots S)_{min}^{35K} = 6.425$ Å; $d(S\cdots S)_{min}^{100K} = 6.457$ Å

d9

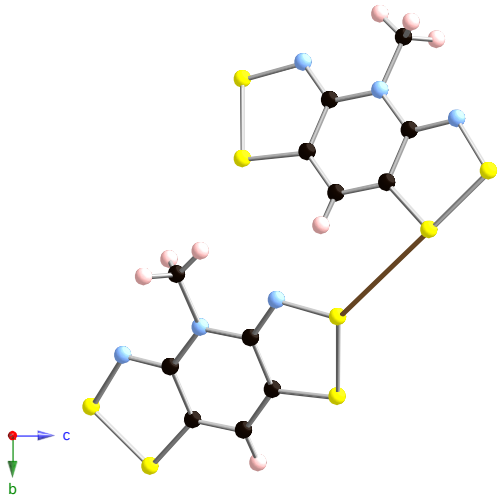

$d(S\cdots S)_{min}^{35K} = 4.310$ Å; $d(S\cdots S)_{min}^{100K} = 4.299$ Å

d10

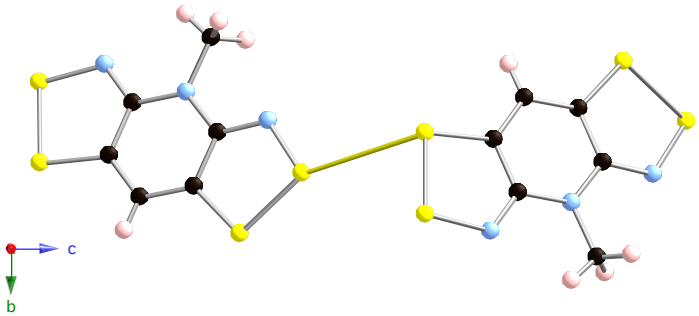

$d(S\cdots S)_{min}^{35K} = 3.641$ Å; $d(S\cdots S)_{min}^{100K} = 3.684$ Å

Table S1. All significant N···N and S···S distances in each pair of BDTMe radicals at 35K and 100K are listed. Also the corresponding J_i value and color code are given for the ten selected dimers (d1-d10).

distance /Å	**d**1 35K (100K)	**d**2 35K (100K)	**d**3 35K (100K)	**d**4 35K (100K)	**d**5 35K (100K)
N···N central ring	10.039 (9.925)	7.521 (7.537)	9.583 (9.552)	3.882 (3.898)	8.840 (8.927)
S···S	3.355 (3.361)	3.337 (3.334)	3.329 (3.325)	3.779 (3.776)	5.817 (5.843)
	3.673 (3.657)	4.808 (4.778)	3.633 (3.627)	3.882 (3.898)	6.371 (6.364)
	3.981 (3.928)				6.978 (7.022)
J_i /cm^{-1}	5.59 (5.78)	-0.61 (-1.11)	2.68 (2.48)	8.81 (4.83)	-0.15 (-0.14)
color code	blue	turquoise	green	red	purple

distance /Å	**d**6 35K (100K)	**d**7 35K (100K)	**d**8 35K (100K)	**d**9 35K (100K)	**d**10 35K (100K)
N···N central ring	7.765 (7.797)	10.746 (10.674)	11.442 (11.353)	8.070 (8.019)	9.917 (9.947)
S···S	7.367 (7.382)	5.996 (5.973)	6.425 (6.457)	4.310 (4.299)	3.641 (3.684)
	7.765 (7.797)	6.553 (6.568)	6.435 (6.459)	4.660 (4.613)	4.045 (4.103)
			6.953 (6.919)	5.982 (5.963)	5.297 (5.346)
***J_i* /cm^{-1}**	0.01 (<|0.05|)	-0.05 (<|0.05|)	-0.04 (<|0.05|)	-0.59 (-0.87)	0.69 (-0.30)
color code	gray	gray	gray	brown	yellow

According to Table S1, the largest change in J_i involves d4 and d10 pairs of radicals. Analyzing the geometry of d4 dimer, one realizes that the two radicals are almost eclipsed since there are 4 S···S and 1 N···N distances equal (3.882Å at 35K and 3.898Å at 100K). It thus follows that J_4 value should decrease because overall at 100K BDTMe radical centers are further apart than at 35K (J_4^{100K}=4.83 cm^{-1} vs. J_4^{35K}=8.81 cm^{-1}). The same applies to J_{10}, for which its J exchange interaction value decreases ~1cm^{-1} and becomes antiferromagnetic (J_{10}^{100K}=−0.30 cm^{-1} vs. J_{10}^{35K}=0.69 cm^{-1}).

Recently we have proved that for the DTA-family of compounds, small changes in distance and angles induce significant changes in *J* exchange interaction value (see magneto-structural correlation maps in T. Francese, J. Ribas-Arino, J.J. Novoa, R.W.A. Havenith, R. Broer, C. de Graaf, M. Deumal, *Phys. Chem. Chem. Phys.* 2018, **20**, 20406). Therefore, the results obtained for BDTMe are not surprising. Once more, these data point out that the *J* exchange interaction dependency on the geometry is exceedingly complex.

Section 2. Comparison between values of J_i from our calculations and from ref. S.M. Winter, *et al. Chem. Commun.* 2009, 7306-7308

The value of the J_i magnetic interaction for all ten selected pairs of BDTMe radicals has been calculated at UB3LYP/6-311++G(d,p) level of theory using the coordinates directly extracted from the crystallographic CIF file at 35K and 100K. Previous work by Winter et al. did also evaluate some of our selected BDTMe dimers using the same DFT functional but a basis set that did not account for diffuse functions, i.e. at UB3LYP/6-311G(d,p) level. The use of diffuse functions provides flexibility to the atomic orbitals that are far away from the nucleus. These functions are advised to be useful when you have a system with expected long-range interactions, i.e. hydrogen bonds, ligand field, or Rydberg states if you compute electronically excited states. The value of J_i is calculated as the energy difference between the open-shell singlet and triplet states using two BDTMe radicals. Accordingly, all intra- and inter-molecular interactions must be adequately described in order to calculate realistic energies. Therefore, in this case the use of diffuse functions is recommended. As Table S2 shows, the introduction of diffuse functions changes the numerical value of the J_i pair exchange interactions but not their magnetic character.

Table S2. Calculated J_i magnetic interactions between BDTMe radicals using 35K and 100K crystallographic data at UB3LYP level using basis sets with (6-311++G(d,p), this paper) and without (6-311G(d,p), Winter, S.M.; *et al. Chem. Commun.* **2009**, 7306-7308) diffuse functions.

candidate *di*	this paper J_i^{35K} /cm^{-1}	Winter *et al.* J_i^{35K} /cm^{-1}	this paper J_i^{100K} /cm^{-1}	Winter *et al.* J_i^{100K} /cm^{-1}
d1	5.59	5.23	5.78	5.38
d2	-0.61	-0.34	-1.11	-0.85
d3	2.68	2.57	2.48	2.39
d4	8.81	7.36	4.83	2.56
d5	-0.15	X	-0.14	X
d6	<|0.05|	X	<|0.05|	X
d7	<|0.05|	X	<|0.05|	X
d8	<|0.05|	X	<|0.05|	X
d9	-0.59	X	-0.87	X
d10	0.69	0.54	-0.30	-0.41

Section 3. Discussion on magnetic models

Simple magnetic models were tested in order to understand the magnetic behavior and, then, select the most adequate models that would offer a more realistic view of the complex 3D magnetic topology (all magnetic models must fulfill the requirement that the maximum number of radicals is 16). These simple models consist of: (1) a spin-ladder model including the two strongest ferromagnetic FM interactions J_1 and J_4 (**Model *J_1_4*** in Figure S3.1a for an 8-radical centers), (2) a model involving the π–stack J_4 FM interaction and the three antiferromagnetic AFM interactions J_2, J_5 and J_9 (**Model *J_4_2_5_9*** in Figure S3.1b for a 12-radical centers), and (3) an additional model including all the relevant magnetic interactions (**Model *J_all*** in Figure S3.1c for a 16-radical centers).

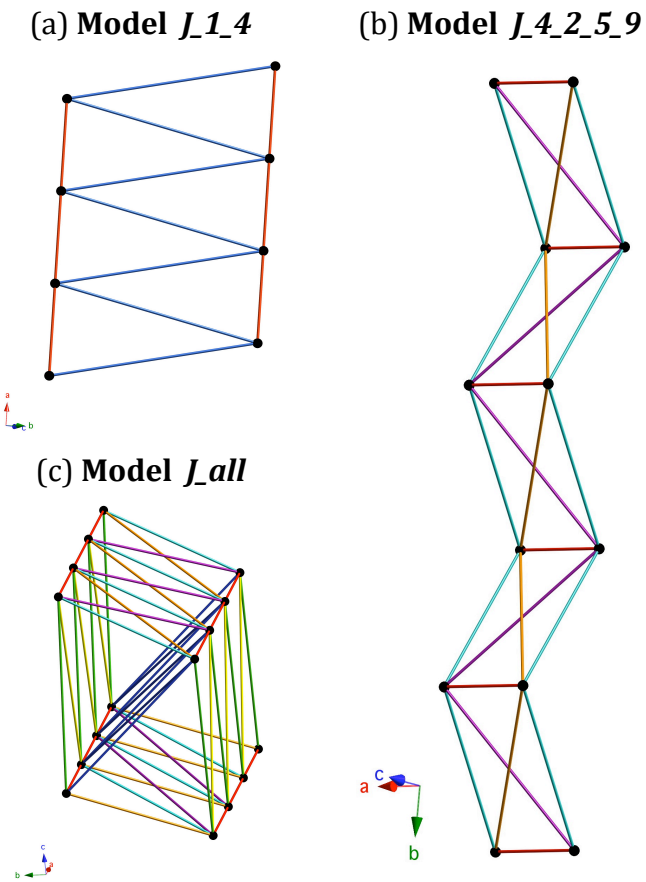

Figure S3.1. (a) 8-radical centers **Model *J_1_4***. (b) 12-radical centers **Model *J_4_2_5_9***. (c) 16-radical centers **Model *J_all***. Color code: J_1 blue, J_2 turquoise, J_3 green, J_4 red, J_5 purple, J_9 brown, J_{10} yellow.

The susceptibility χT(T) curves were calculated using **Model *J_1_4*** and **Model *J_4_2_5_9*** that are enlarged from 4 to 12, and from 6 to 16 radicals, respectively (see Figure S3.2 for zero field and Figure S3.3 for 0.1 Tesla). However, they did not reproduce correctly the experimental results since they were not able to describe appropriately the 3D magnetic topology of the BDTMe crystal.

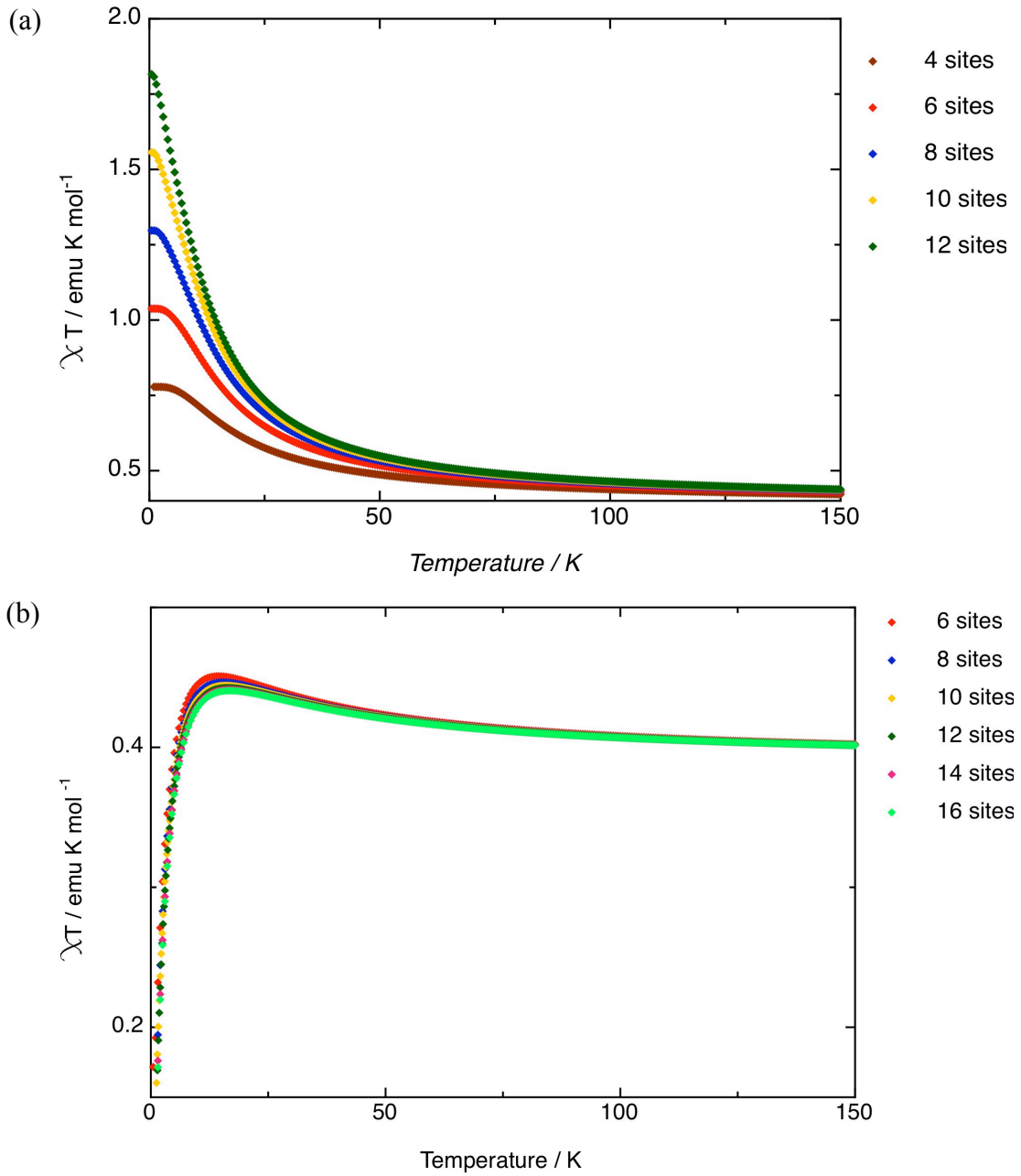

Figure S3.2. Susceptibility χT(T) curves using (a) **Model *J_1_4*** being enlarged from 4 to 12 radicals, and (b) **Model *J_4_2_5_9*** being enlarged from 6 to 16 radicals.

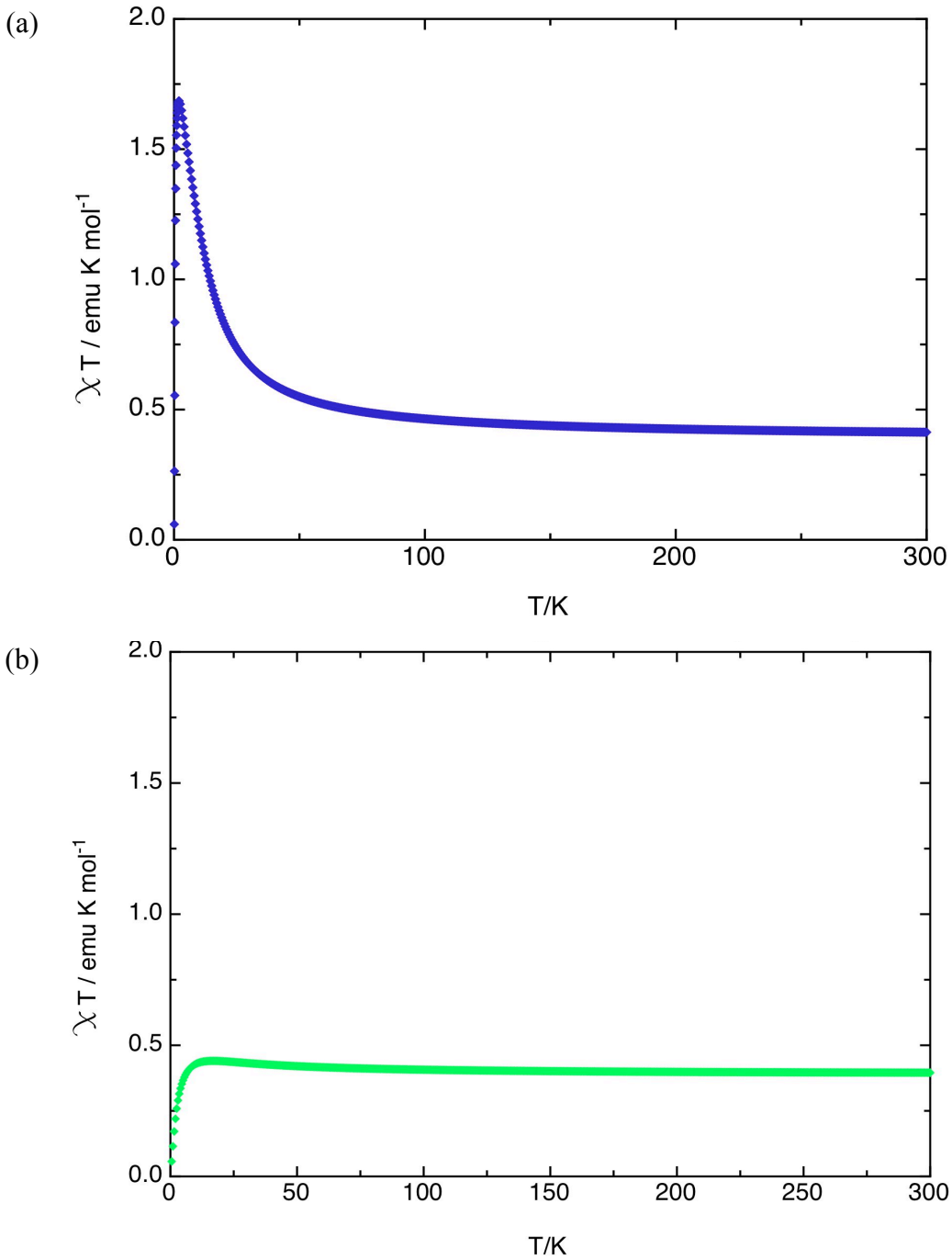

Figure S3.3. Magnetic susceptibility χT(T) using (a) **Model J_1_4** with 12-radical centers, and (b) **Model J_4_2_5_9** with 16-radical centers, at a magnetic field of 0.1 Tesla.

Further calculations of χT(T) using **Model *J_all*** were not able to reproduce the experimental data (see Figure S3.4).

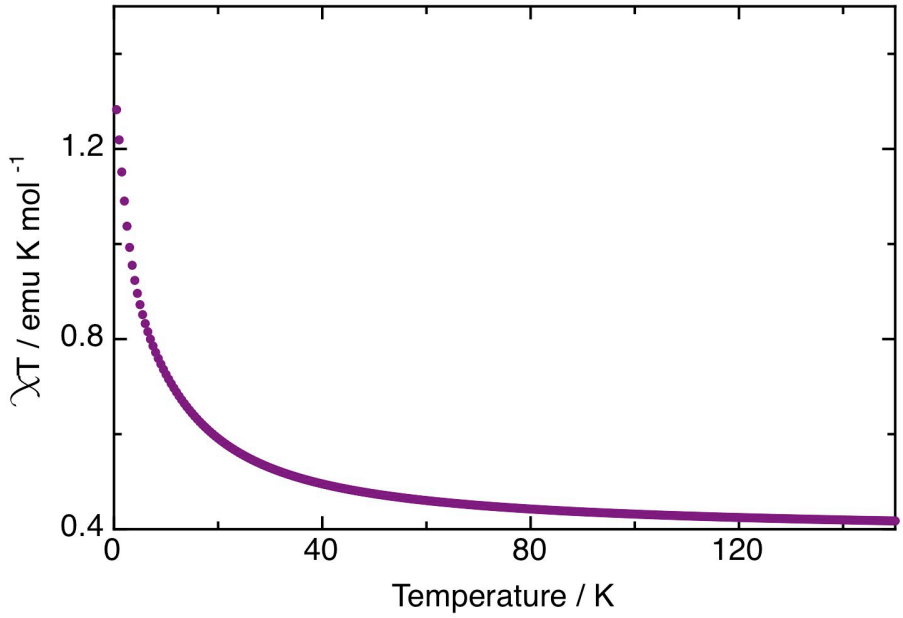

Figure S3.4. Magnetic susceptibility χT(T) using **Model J_all** with 16-radicals.

Finally, two models were chosen (see Figure S3.5a), both of them containing 16 radical molecules and the important magnetic interactions collected in Table S1. The first 2(4+4) model accounts for 2 connected spin ladders to consider the effect of the number of π-stacked radicals (*a*-axis). Each spin ladder has 4-radicals along the rail direction. The second 4(2+2) model accounts for 4 connected spin ladders and is meant to explore the cooperativity introduced by J_3. Comparison between the experimental data and the computed magnetic susceptibility χT as a function of temperature for the two models using Statistical Mechanics shows that the high temperature region is described correctly, and there is a reasonable description at low temperatures. For the 2(4+4) model (Figure S3.5a, top), the π-stack J_4 rail (the strongest FM interaction) and J_1 rung interactions propagate. As a consequence, the χT curve rises at higher temperatures compared to the 4(2+2) model (Figure S3.5a, bottom). Further, according to Figure S3.5b, the slope of the χT curve using the 4(2+2) model resembles much more the experimental curve, although there is a temperature lag to reach the maximum χT value. Therefore, although the magnetic model has limitations, the analysis of the χT curves enables to conclude that the 4(2+2) model reproduces better the experimental results.

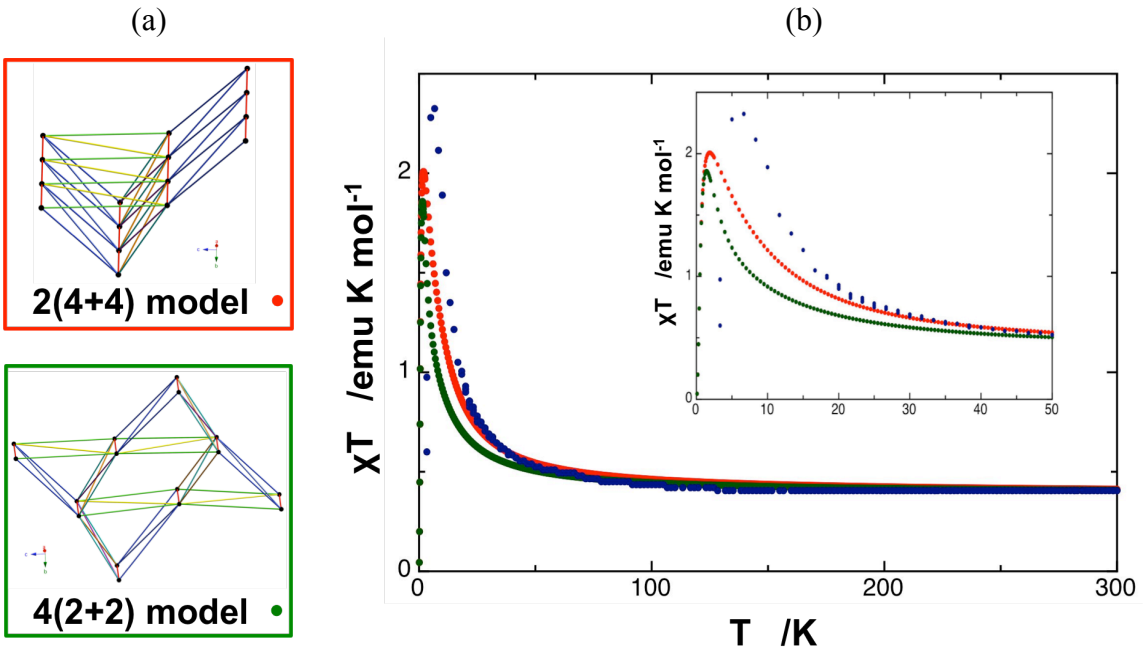

Figure S3.5. (a) Magnetic 2(4+4) and 4(2+2) models. (b) χT(T) plots at H=0.1T for the 2(4+4) model (red), the 4(2+2) model (green), and the experimental data (blue) for temperatures from 0-300K. Inset view a zoom for the 0-50K range of temperatures.